

# RECLAMATION

*Managing Water in the West*

**Desalination and Water Purification Research  
and Development Program Report No.126**

## **Molecular Basis of Reverse Osmosis Membrane Biofouling: Analysis of the Membrane Adsorption Behavior of Bacterial Alginate, a Model Extracellular Substance**



**U.S. Department of the Interior  
Bureau of Reclamation  
Technical Service Center  
Denver, Colorado**

May 2006

REPORT DOCUMENTATION PAGE			Form Approved OMB No. 0704-0188		
The public reporting burden for this collection of information is estimated to average 1 hour per response, including the time for reviewing instructions, searching existing data sources, gathering and maintaining the data needed, and completing and reviewing the collection of information. Send comments regarding this burden estimate or any other aspect of this collection of information, including suggestions for reducing the burden, to Department of Defense, Washington Headquarters Services, Directorate for Information Operations and Reports (0704-0188), 1215 Jefferson Davis Highway, Suite 1204, Arlington, VA 22202-4302. Respondents should be aware that notwithstanding any other provision of law, no person shall be subject to any penalty for failing to comply with a collection of information if it does not display a currently valid OMB control number. PLEASE DO NOT RETURN YOUR FORM TO THE ABOVE ADDRESS.					
1. REPORT DATE (DD-MM-YYYY) 2006		2. REPORT TYPE Final		3. DATES COVERED (From - To) October 31, 2004 - December 31, 2005	
4. TITLE AND SUBTITLE Molecular Basis of Reverse Osmosis Membrane Biofouling: Analysis of the Membrane Adsorption Behavior of Bacterial Alginate, a Model Extracellular Substance			5a. CONTRACT NUMBER Agreement No. XXX		
			5b. GRANT NUMBER		
			5c. PROGRAM ELEMENT NUMBER		
6. AUTHOR(S) Martin Reinhard, Harry Ridgway and Eva Steinle-Darling			5d. PROJECT NUMBER		
			5e. TASK NUMBER		
			5f. WORK UNIT NUMBER		
7. PERFORMING ORGANIZATION NAME(S) AND ADDRESS(ES) Stanford University, 450 Serra Mall, Stanford, CA 94305			8. PERFORMING ORGANIZATION REPORT NUMBER		
9. SPONSORING/MONITORING AGENCY NAME(S) AND ADDRESS(ES) Bureau of Reclamation U.S. Department of the Interior Denver Federal Center PO Box 25007, Denver, CO 80225-0007			10. SPONSOR/MONITOR'S ACRONYM(S) Reclamation		
			11. SPONSOR/MONITOR'S REPORT NUMBER(S) DWPR Report No. 126		
12. DISTRIBUTION/AVAILABILITY STATEMENT Online at <a href="https://www.usbr.gov/research/dwpr/DWPR_Reports.html">https://www.usbr.gov/research/dwpr/DWPR_Reports.html</a>					
13. SUPPLEMENTARY NOTES					
14. ABSTRACT Biofouling continues to be an impediment to the application of reverse osmosis (RO) technology. This project was to determine correlations between the static adsorption behavior of the model foulant bacterial alginate, membrane characteristics, and membrane performance data to obtain a predictive metric of membrane fouling potential. C-labeled bacterial alginate produced by mucoid strains of <i>Pseudomonas aeruginosa</i> was harvested, purified and used in static adsorption experiments on four RO membrane types. While these results alone are not enough to determine which membrane characteristics are important for membrane bio-fouling and will have to be corroborated by cross-flow fouling experiments under the same conditions, they do point to some general trends: desorption kinetics may be a good indicator of general fouling behavior, membrane or coating surface roughness is not as good an indicator of fouling behavior as generally thought, and some water molecules initially associated with the alginate chain rapidly exchanged with membrane waters of hydration resulting in partial dehydration of the alginate. Further exploration and quantification of the later phenomenon may help elucidate how bacterial alginate and other adsorbed polymeric foulants affect membrane water flux.					
15. SUBJECT TERMS Membrane, fouling, biofilm, desalination					
16. SECURITY CLASSIFICATION OF:			17. LIMITATION OF ABSTRACT	18. NUMBER OF PAGES 29	19a. NAME OF RESPONSIBLE PERSON Yuliana Porras-Mendoza
a. REPORT U	b. ABSTRACT U	THIS PAGE U			19b. TELEPHONE NUMBER (Include area code) 303-445-2265

Grant # 04-Fc-81-1045A  
Bureau of Reclamation

Molecular Basis of Reverse Osmosis Membrane  
Biofouling: Analysis of the Membrane Adsorption  
Behavior of Bacterial Alginate, a Model Extracellular  
Substance

Martin Reinhard, Harry Ridgway and Eva Steinle-Darling

Submitted to:  
Andrew Murphy  
Bureau of Reclamation  
PO Box 25007, DFC  
Mail Code: D-78  
Denver, CO 80225-0007

Performance Period: October 31, 2004 - December 31, 2005  
Date: May 24, 2006

# 1 Acknowledgements

This work was partially supported by the National Science Foundation under agreement number CTS-0120978. Membranes were donated by Hydranautics (Oceanside, CA), and coatings were provided by Membrane Technology and Research (Menlo Park, CA).

# 2 Abstract

Biofouling continues to be an impediment to the application of reverse osmosis (RO) technology for large-scale water recycling and is therefore an intensive field of study. Biofilms form on RO membranes through transport of cells to the membrane surface where they undergo adhesion and multiplication. Extracellular polymeric substances (EPS) secreted by the cells form a major component of most biofilm matrices and help stabilize their structure. Bacterial alginate is among the best-studied examples of EPS. In this project, the goal was to determine correlations between the static adsorption behavior of the model foulant bacterial alginate, membrane characteristics, and membrane performance data in order to obtain a predictive metric of membrane fouling potential.

To this end,  $^{14}\text{C}$ -labeled bacterial alginate produced by mucoid strains of *Pseudomonas aeruginosa* was harvested, purified and used in static adsorption experiments on four RO membrane types: virgin ESPA-3, coated ESPA-3 (PEBAX 1657), LFC-3 and SWC-4. The adsorptions of alginate onto virgin ESPA-3, PEBAX-coated ESPA-3 and LFC-3 were nearly within one standard deviation of one another ( $42.6 \pm 11.4$ ,  $38.5 \pm 14.7$ ,  $53.9 \pm 13.8$  mg/m<sup>2</sup>, respectively, after 24h contact with 1 g/L alginate solution) and therefore statistically not different from one another. The adsorption of alginate onto SWC-4, on the other hand, was approximately five times less ( $8.4 \pm 4.4$  mg/m<sup>2</sup> after 24h at 1 g/L).

On the other hand, the desorption kinetics were markedly different. While the desorption experiments resulted in only slightly more differentiated equilibrium results, with 55%, 73%, 71%, and 90% irreversible sorption for ESPA-3, LFC-3, PEBAX-coated ESPA-3 and SWC-4, respectively, the kinetic desorption behavior was more in line with the expected low-fouling behavior of LFC-3: This membrane showed an approximate first-order desorption time constant of 3h, as opposed to more than 15h for both ESPA-3 (17h) and PEBAX-coated ESPA-3 (27h). The desorption kinetics for SWC-4 were not determined due to its high degree of irreversible fouling.

While these results alone are not sufficient to determine which membrane characteristics are important for membrane bio-fouling and will have to be corroborated by cross-flow fouling experiments under the same conditions, they do point to some general trends: First, LFC-3, which is sold as a low-fouling membrane, experienced a similar amount of alginate adsorption as the virgin ESPA-3, and retained similar amounts of alginate after desorption of the reversible fraction. However, the desorption kinetics were almost instantaneous for the low-fouling LFC-3, whereas the desorption time constants for the other membranes were

an order of magnitude higher. Therefore, desorption kinetics may be a good indicator of general fouling behavior. Also, more irreversible fouling was observed on the much smoother PEBA-coated ESPA-3 [7] than on the virgin surface of the same membrane. This is contradictory to other previous findings involving oil-water emulsions [7], and might indicate that membrane or coating surface roughness is not as good an indicator of fouling behavior as generally thought.

A molecular dynamics (MD) simulation was performed to explore how an acetylated bacterial alginate foulant might undergo adsorption to a “standard” fully aromatic crosslinked polyamide (PA) reverse osmosis (RO) membrane. Computer algorithms were written or modified to automate building of separate alginate and membrane models that were subsequently integrated into a single partially hydrated molecular system. An MD simulation was run for  $\sim 300$  psec ( $\sim 0.3$  ns) at a constant temperature of 300OK. The results suggested that bacterial alginate undergoes gradual adsorption to the PA membrane surface with a net potential energy change of about -1200 kcal/mol. Both the alginate polymer and the membrane surface appeared to undergo mutual conformational rearrangements leading to a low-energy “dovetailing” of the molecules possibly involving acetyl substitutions on the alginate. Although electrostatic interactions clearly dominated the adsorption process, non-bond Van der Waals interactions became more significant as alginate atoms approached within several Angstroms of the membrane surface. In addition, some water molecules initially associated with the alginate chain rapidly exchanged with membrane waters of hydration resulting in partial dehydration of the alginate. Further exploration and quantification of the later phenomenon may help elucidate how bacterial alginate and other adsorbed polymeric foulants affect membrane water flux.

### 3 Background

Reverse osmosis (RO) has a great potential to provide very pure water from marginal quality water (either saltwater or reclaimed wastewater) on a large scale. The main impediment to the larger-scale implementation of RO for drinking water recovery is the cost associated with membrane cleaning and replacement, as well as increasing operating pressures. All these factors are due to the membrane fouling with a variety of substances, in particular biofilms.

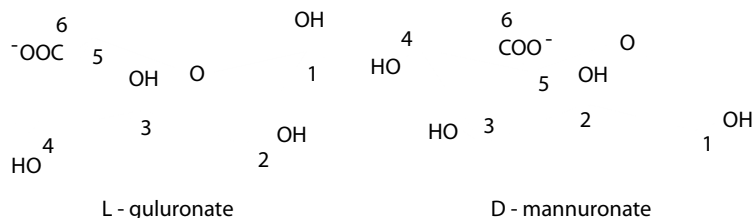


Figure 1: Chemical structure of the monomers in bacterial alginate. Acetylation may occur at the 2 and 3 positions on mannuronate.



## 4 Alginate Growth and Purification

To this end, mucoid strains of *Pseudomonas aeruginosa*, known for their copious alginate production, were obtained from the Mike Franklin at the Center for Biofilm Engineering at Montana State University. These strains were cultured on  $^{14}\text{C}$ -labeled glycerol. The alginate was then harvested and purified following a procedure similar to those described previously [9], [4], and as outlined by a procedure obtained from Michael Franklin personally [3]. In addition to the standard procedure, the medium is radio-labeled with  $^{14}\text{C}$ , such that adsorption data can be read via a liquid scintillation counter:

**Day 1 (Fri-Mon)** Grow on radio-labeled glycerol medium for 2-3 days at  $37^\circ\text{C}$  on a shaker. Medium will have 1 mCi/L.

**Day 4: (Mon)** Precipitate alginate from the cultures by adding 3-4g/L of cetylpyridinium chloride (CPC) (Sigma - C0732). Centrifuge at 10,000 rpm for 10-15 min to isolate precipitated alginate. Resuspend (overnight at  $37^\circ\text{C}$  on a shaker) in 1/3 original volume of 1M NaCl.

**Day 5: (Tue)** Precipitate out alginate with equal volume of isopropyl alcohol. Resuspend (overnight at  $37^\circ\text{C}$  on a shaker) in 1/3 original volume of 0.85% NaCl.

**Day 6: (Wed)** Centrifuge to remove cell debris. Add NaCl to bring to an approximate total concentration of 1M. Precipitate with an equal volume IPA. Centrifuge to isolate alginate pellets. Wash extensively with 50% IPA/ 50% deionized water. Resuspend in small volume of deionized water. Place in oven at  $50^\circ\text{C}$  to dry. This takes much longer than the “overnight”, on the order of a week.

**Days later:** Once the alginate is dry, scrape it out using a small spatula and place flaky powder into a new vial. Add  $\sim 10\text{mL}$  of deionized water to the old vial and let shake overnight at  $37^\circ\text{C}$ . Repeat from last step of Day 6.

In total, approximately 100 mg of labeled wild-type alginate have been produced, with an approximate activity of  $50 \mu\text{Ci/g}$ .

In the proposal and previous progress reports, further purification of the alginate preparation was discussed. This involved the additional steps of incubating the alginate solution with pronases and nucleases in order to digest any proteins or polynucleic acids present, followed by extensive dialysis against deionized water. This approach, however, led to an unacceptable drop in alginate yield from the procedure. Therefore, the effectiveness of these last steps were examined using a standard protein assay (Pierce, BCA Protein Assay Kit) and it was found that the alginate pre-digestion was already pure to 99.2 m% and that the digestion only increased this to 99.4 m%. Hence, the decision was made to drop the digestion and dialysis steps from the purification procedure.

## 5 Adsorption and Desorption Assay Procedure

The adsorption assay for alginate is based on a similar adhesion assay performed with live bacteria, to measure the extent of bacterial adhesion to different membrane types [1]. However, this procedure requires even less solution, such that many measurements can be made with very little labeled alginate.

### 5.1 Adsorption Assay

Figure 3 on page 6 shows a schematic of the Alginate Adsorption Assay. In this procedure, the wells in a commercially available 24-well microtiter plate are filled with 1.5-2 mL of 0.8% purified agarose solution, which forms a rigid gel once cooled. Membrane coupons ( $\text{Ø} = 9.5$  mm), soaked in deionized water for 24h prior to experimentation, are placed in each well on top of the gel, which serves to keep them hydrated. Finally, glass fiber filter pads (GFP,  $\text{Ø} = 7.9$  mm) are plated on top of the membrane coupons, taking care that they are placed in the center, such that an intact ring of membrane coupon is visible around the GFP.

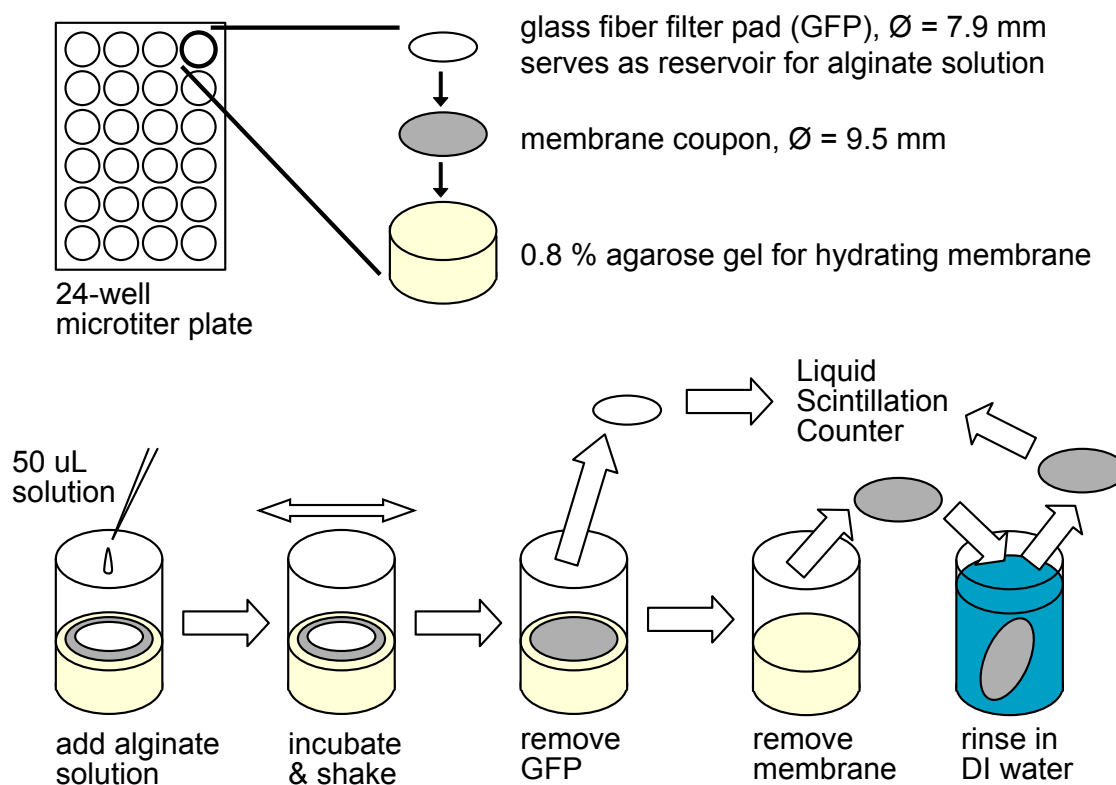


Figure 3: Schematic of the Alginate Adsorption Assay

To begin the experiment, 50  $\mu\text{L}$  of alginate solution of a known concentration are pipetted directly onto the GFP, which is at this point completely saturated with solution. It will

therefore act as a reservoir of alginate solution for the duration of the experiment, *without allowing any solution to contact the sides, or back of the membrane coupon*. Therefore, the area of interest in terms of adsorption,  $A$ , is that covered by the GFP, so  $A = \frac{\pi}{4}(7.9\text{mm})^2$ .

The experiment proceeds by placing the entire plates onto an orbital shaker at 100rpm to enhance mass transfer rates. After the desired time has elapsed, the GFP pad is removed from the well and placed into a liquid scintillation (LS) vial. Then, the membrane coupon is removed. Excess solution clinging to the membrane surface, as well as any very loosely-bound alginate is rinsed off by dipping the coupon three times in deionized water. Then it is placed into another LS vial. The activity of both the GFP and the membrane coupon are counted on the liquid scintillation counter (LSC).

From calibration data (counting known volumes of alginate solution with known concentration), the conversion factor between the disintegration per minute (DPM) activity reading from the LSC and the mass of alginate can be calculated. Since different batches of alginate may have different values of activity per mass, and there may even be heterogeneities within a single batch, these calibrations are performed for each new solution prepared. Once the activity per mass is known, the DPM data can then be further translated into the mass adsorption per unit area through the known quantity of  $A$ .

To alleviate concerns that pure solution activity would read differently than that of solution sorbed to a membrane coupon or GFP, the first set of calibration data included samples that contained a GFP that had been placed directly into an LS vial, and then saturated with a known volume of alginate solution. The activities of 50  $\mu\text{L}$  alginate solution sorbed to a GFP and 50  $\mu\text{L}$  alginate solution without any “interferences” were within the error of the instrument, which is orders of magnitude smaller than the variations found in the adsorption data.

## 5.2 Desorption Assay

The procedure for the desorption experiments is very like the procedure for the adsorption experiments described in Section 5.1. With the setup remaining identical, all the membranes are exposed to a 1 g/L alginate solution for 24 h via a GFP soaked in said solution. Figure 4 on page 8 shows the remaining steps, as described here: After the 24 h adsorption time has elapsed, the GFP is removed and replaced with a fresh GFP, which is then soaked with 50  $\mu\text{L}$  of deionized water. The desorption time begins at this point, following which samples are taken and processed as before. Additionally, for a smaller subset of samples, the second set of GFPs, as well as the activity of the rinse water are also counted in order to calculate a mass balance on the total amount adsorbed. In all cases measured, the total mass was recovered between the three media (GFPs, rinse water and membrane coupon) to within the error bounds on the original adsorption values.

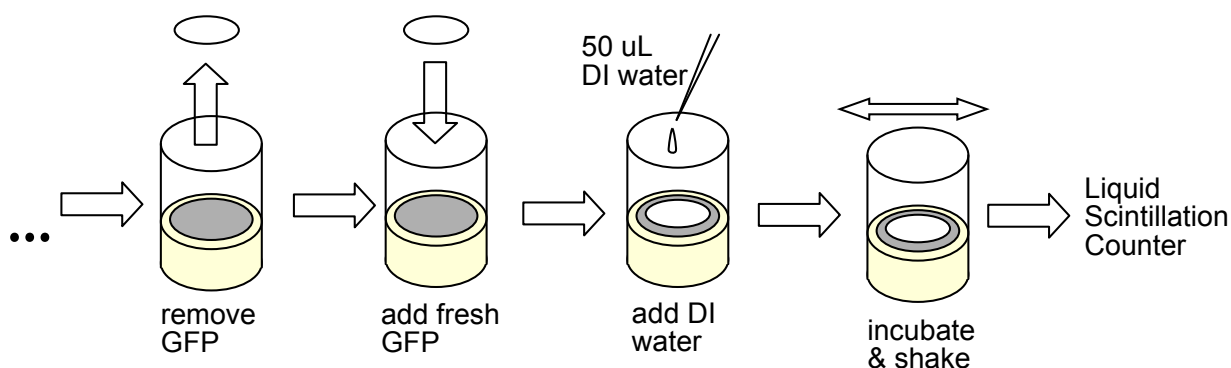


Figure 4: Schematic of the desorption portion of the Alginate Desorption Assay

## 6 Assay Verification

One concern with the adsorption procedure as outlined in the previous section is the competition between the glass fibers in the GFPs competing for the alginate as an adsorbing surface. A control experiment using the colorimetric method described in the next section showed the adsorption to the GFPs to be negligible, as described in section 6.2.

### 6.1 Phenol Sulfuric Acid Method

The Phenol-Sulfuric Acid Method is a well-known way to measure aqueous carbohydrate concentrations [5], [8]. This method is based on the reaction of phenol with hexoses and pentoses to form an orange-yellow adduct under strong acidic conditions. Through rapid addition of concentrated sulfuric acid, more complex carbohydrates, such as alginate, are completely hydrolysed to pentose and hexose monomers, which then can also undergo complete phenol addition [6]. In the absence of other interfering carbohydrates, this method is therefore a quick and easy procedure to determine alginate concentrations in solution.

We followed the procedure outlined by Saha and Brewer [6], with the exception of measuring light absorption at 480nm, the specific absorbance peak for uronic acids [8], instead of the more generic peak at 488-490nm [5], [6]. Figure 5 on page 9 shows a calibration curve produced with bacterial alginate solutions. The linearity of the data indicates that this method is accurate at the concentrations tested. Also, the data in Fig 5 were collected on different occasions, showing consistency over time. This method is therefore be a valuable tool in determining aqueous alginate concentrations.

### 6.2 Control Experiment: Alginate Adsorption onto GFP Material

After the completion of some of the membrane adsorption experiments, we were asked whether alginate is being sorbed onto the glass fibers in the glass fiber filter pads (GFPs) during the membrane adsorption experiments. This would bias the experimental results,

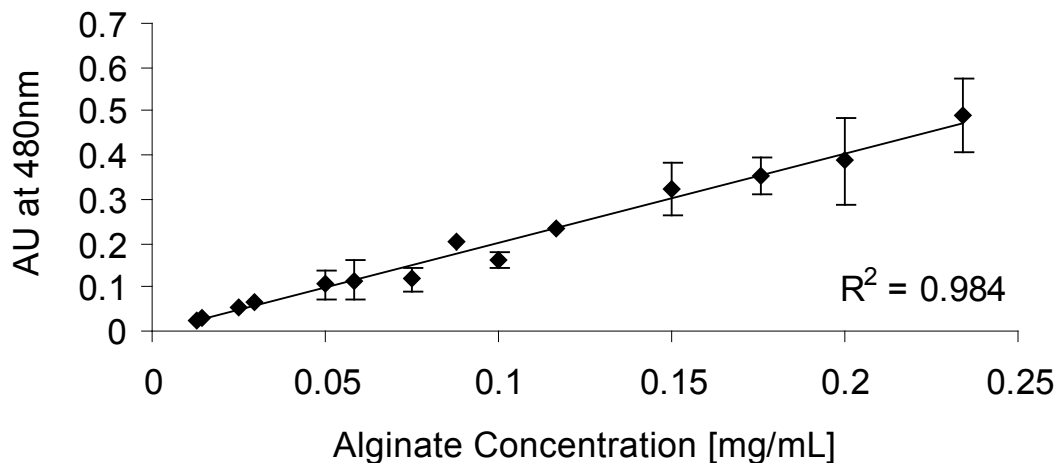


Figure 5: Calibration curve for Phenol Sulfuric Acid Method using bacterial alginate. Data points shown are the average of three measurements, error bars represent one standard deviation. If no error bars are shown, the standard deviation is smaller than the symbol.

since the actual concentration of alginate in contact with the membrane surface could be lower than expected. The purpose of this experiment was to dispel any concerns over a change in bulk concentration of alginate during the membrane adsorption experiments.

The concept was to place GFPs in solutions of known concentration and measure the change in concentration in the solutions before and after contact with the GFPs. Since we were measuring the sorbed alginate by difference in the aqueous concentration, it can be done colorimetrically (without the use of valuable  $C^{14}$ -labeled alginate) via the Phenol Sulfuric Acid Method as described in section 6.1.

For each sample replicate, 5 mL alginate solution was placed into a 20-mL capped glass vial and allowed to equilibrate for 24h. Then a 50  $\mu$ L sample was taken to measure the starting concentration. 170mg of GPF material, cut into pieces of a similar size as the  $\varnothing=$  7.9 mm pads from the membrane adsorption experiments, were added to each vial. The vials were capped and placed on an orbital shaker at approximately 100 rpm for over 24h at room temperature. Then, another 50  $\mu$ L sample was taken from each vial. All samples were diluted 10-fold with deionized water and then analyzed using the method described in Section 6.1. The difference between the alginate concentrations before and after exposure to GFPs was then converted to a percentage of the original concentration, in order to compare all measurements.

This setup mimics experimental conditions from membrane adsorption studies as closely as possible, since similar alginate solution concentrations (0.25-1.35 g/L) and a ratio of GFP material to alginate solution (0.11 g/mL) as similar as possible to the actual membrane adsorption experiments (0.034 g/mL) were used. This ratio is larger for the control experiment than for actual membrane adsorption experiments because enough supernatant was needed to be able to sample the solutions after contact without interference from the GFP material, whereas supernatant is explicitly undesired for the membrane adsorption experiments, for reasons described in Section 5.

In total, 24 replicates at 8 different concentrations were measured before and after contact with GFP material. The mean adsorption of alginate was 3.2% with a standard deviation of 6.7%. Within the precision of our method, there is therefore no significant adsorption of alginate onto the GFP material, and therefore no bias in the membrane adsorption data from this source.

## 7 Membrane Types

Several adsorption experiments have been performed since the beginning of September. They were performed on three different reverse osmosis membranes, all manufactured by Hydranautics, ESPA-3, LFC-3 and SWC-4. The ESPA-3 is one of four membranes in the ESPA (Energy Saving PolyAmide) line, which is designed for high flux and medium rejection. This makes them applicable mainly for brackish water. LFC-3 is a member of the LFC (Low Fouling Composite) family, which is sold as a low-fouling alternative to ESPA, in particular for water recycling applications. The SWC (SeaWater Composite) membranes are high-pressure, high-selectivity membranes. As the name suggests, they are used in seawater desalination.

In addition to the three commercial RO membranes, the adsorption experiments were performed on a surface-coated version of the ESPA-3 (coating provided by Membrane Technology and Research, Mountain View, CA), which was dip-coated in a 1% PEBAX solution. PEBAX is hydrophilic polyamide-polyether block copolymer (Pebax 1657, Atofina, Philadelphia, PA). AFM images of the uncoated and coated ESPA-3 taken by other researchers in the Reinhard group show that the coated version is much smoother [7].

## 8 Adsorption Assay Results

### 8.1 Kinetic Data

Kinetic data was the first to be collected using the new Adsorption Assay. Therefore, the first few sets of data collected were inconsistent and not representative due to procedural errors. The data shown in Figure 6 is the result of the kinetic experiment deemed most reliable due to a lack of procedural errors, as well as consistency with data from isotherm and desorption experiments. This experiment was run simultaneously for all four membrane types described in Section 7.

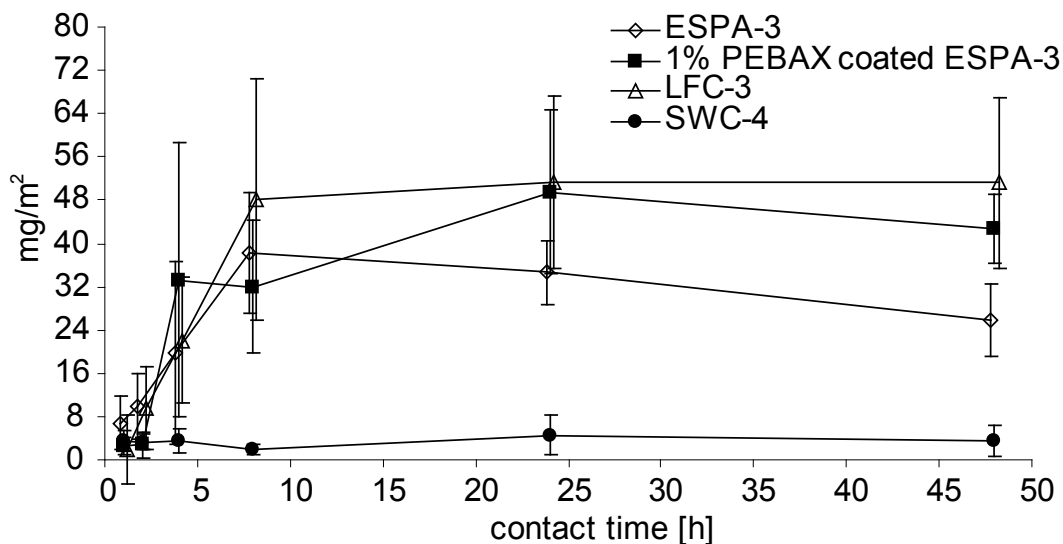


Figure 6: Adsorption Kinetics for a 1g/L Bacterial Alginate solution. Data points are the average values of eight replicates, error bars represent one standard deviation.

Despite the large variance in the data shown in Figure 6, two important observations can be made: First, while ESPA-3, 1% PEBAX-coated ESPA-3 and LFC-3 behave nearly within error bounds of each other at all times, SWC-4 shows almost an order of magnitude less alginate adsorption than the others. Secondly, and more importantly, the data show clearly that equilibrium has long been reached once the contact time reaches 24h. Knowing this, we can safely move on to isotherm experiments with on the order of 24h of contact time.

## 8.2 Isotherm Data

The results from two isotherm experiments can be seen in Figure 7 on page 12. As the figure shows, the two data sets line up within error bounds on all occasions (except for SWC-4, on which no second isotherm measurements were taken).

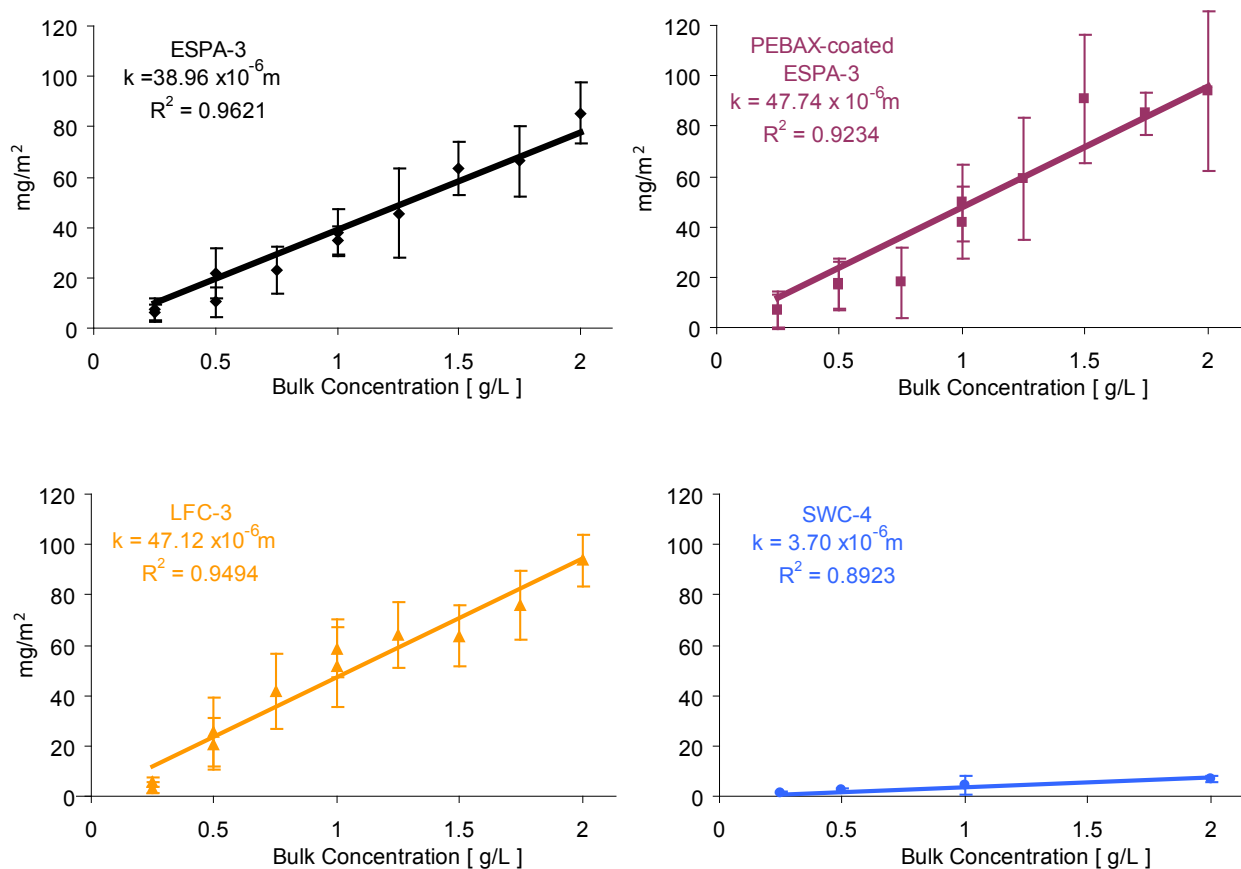


Figure 7: Adsorption isotherms for bacterial alginate on 4 RO Membranes after 24 hours' contact with alginate solutions. Data points are the average values for eight replicates, error bars represent one standard deviation. If no error bars are shown, the standard deviation is smaller than the symbol.

As with the one kinetic experiment that includes all four membranes, it is clear that the SWC-4 membrane adsorbs much less than the other membranes. The other three membrane types are essentially indistinguishable, due to large variations between replicates. However, the relatively small error bars for the SWC-4 membrane indicate that experimental error is not responsible for the larger variations in the measurements of the other three membranes. It is assumed that the variation in adsorption for the looser brackish water membranes is due to their intrinsic surface heterogeneity, which reconfirms the necessity of measuring many replicates per data point to obtain a true mean value for the adsorption over a larger surface area.

## 9 Desorption

While the data collected in adsorption experiments is fundamentally interesting in terms of the affinity of alginate for different surfaces, the more pertinent information with respect to membrane fouling is likely how much of the adsorbed alginate is *irreversibly* adsorbed to the surface. Particularly, the kinetics of desorption are also likely to play a role in a cross-flow situation, since a true (thermodynamic) equilibrium is never reached. Therefore, desorption experiments were performed to determine the irreversible fraction of alginate adsorption as well to determine the kinetics of desorption.

### 9.1 Desorption Data

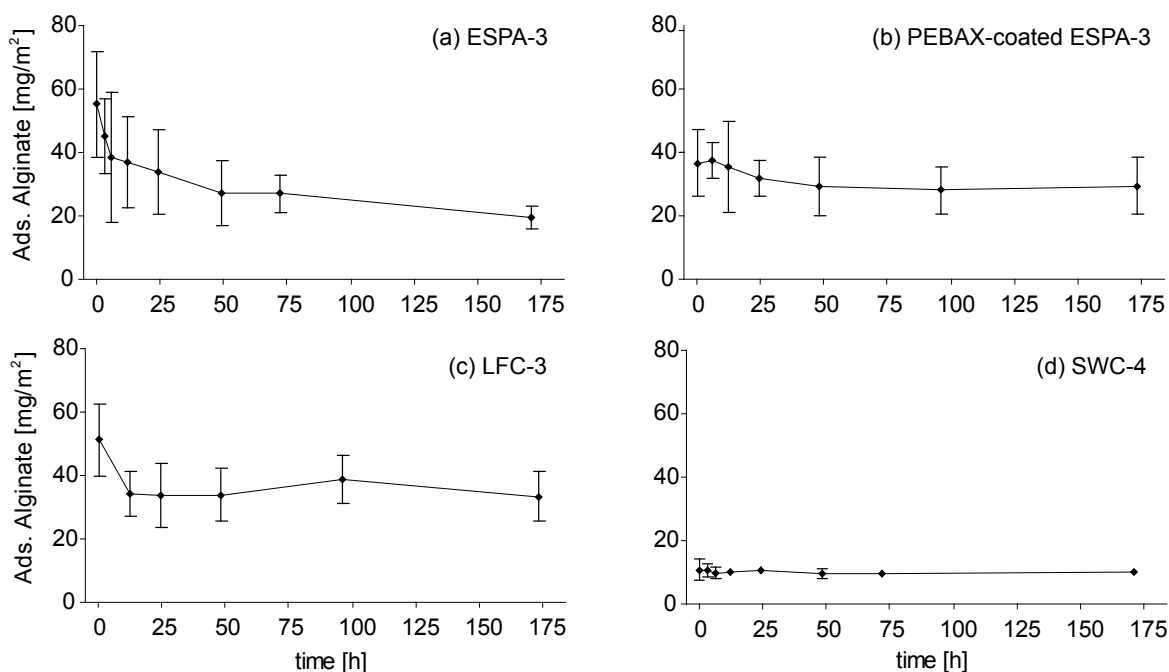


Figure 8: Desorption kinetics for bacterial alginate on 4 RO Membranes after 24 h contact with 1 g/L alginate solution. Data points are the average values for eight replicates, error bars represent one standard deviation. If no error bars are shown, the standard deviation is smaller than the symbol.

Figure 8 shows the data from desorption experiments on all four RO membranes (ESPA-3, PEBAX-coated ESPA-3, LFC-3 and SWC-4) after they were in contact with a 1 g/L alginate solution for 24 h. As before, it is interesting to note the very small amount of adsorption on SWC-4 after 24 h as compared to the other membranes. These data, however, also show significant differences between the membranes that produced very similar data in the adsorption experiments described in Sections 8.1 and 8.2: While the desorption experiments resulted in only slightly more differentiated equilibrium results, with 55%, 66%, 73%, and 89% irreversible sorption for ESPA-3, LFC-3, PEBAX-coated ESPA-3 and SWC-4, respectively,

the kinetic desorption behavior was more in line with the expected low-fouling behavior of LFC-3: This membrane showed an approximate first-order desorption time constant of 3h, as opposed to more than 15h for both ESPA-3 (17 h) and PEBAX-coated ESPA-3 (27 h).

## 9.2 Desorption Model

A simple first-order desorption model serves to quantify three parameters relevant to alginate fouling of membrane surfaces, as shown in Equation 1: Total initial adsorption ( $A(0) = A_1 + A_2$ ), irreversible adsorption ( $A_2$ ) and a time constant for the desorption kinetics ( $\tau$ ).

$$A(t) = A_1 e^{-t/\tau} + A_2 \quad (1)$$

$$\ln(A(t) - A_2) = \ln(A_1) - \frac{1}{\tau}t \quad (2)$$

In order to find the model parameters, a linearized version of Equation 1, shown in Equation 2 is used. Thus, the slope of the plot is  $-\frac{1}{\tau}$ , the and  $\ln(A_1)$  is the intercept. The third parameter,  $A_2$ , is found via iteration to minimize the  $R^2$ -value on the linear fit.

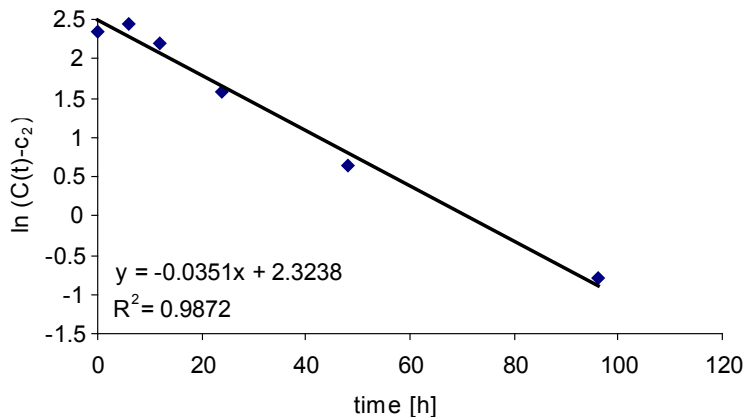


Figure 9: Linearized graph of desorption data for PEBAX-coated ESPA-3 membrane.

An example for the data fit is shown in Figure 9 for a the desorption experiment with PEBAX-coated ESPA-3. As shown, the linearity for this fit is exceptionally good ( $R^2 = 0.98+$ ). The fit for the uncoated ESPA-3 was also acceptable ( $R^2 = 0.92$ ). The lack of as good a linear fit for SWC-4 ( $R^2 = 0.74$ ) is explained handily by the fact that very little desorption was observed at all, and therefore small scatter in the data, especially at earlier times, caused larger deviations from linearity. Finally, LFC-3 data was not fitted according to this method due to reasons described below.

Figure 10 shows the results from the same desorption experiment as shown in Figure 8 with the first-order desorption model expressed by Equation 1 superimposed. For (a), (b) and (d), the model graph was obtained via the linearization method described previously in this section, as shown in Figure 9 for the PEBAX-coated ESPA-3 data. For LFC-3, not enough data were available at  $t < 12$  h, so the model parameters were approximated via inspection. As can be seen in Figure 8 and particularly in Figure 10, the drop to a constant level is achieved at or before the second data point at 12 h. Therefore, not enough data was available to even attempt a linear fit according to Equation 2. Instead, the approximate parameters  $A_1$ ,  $A_2$  and  $\tau$  for LFC-3 were determined by inspection.

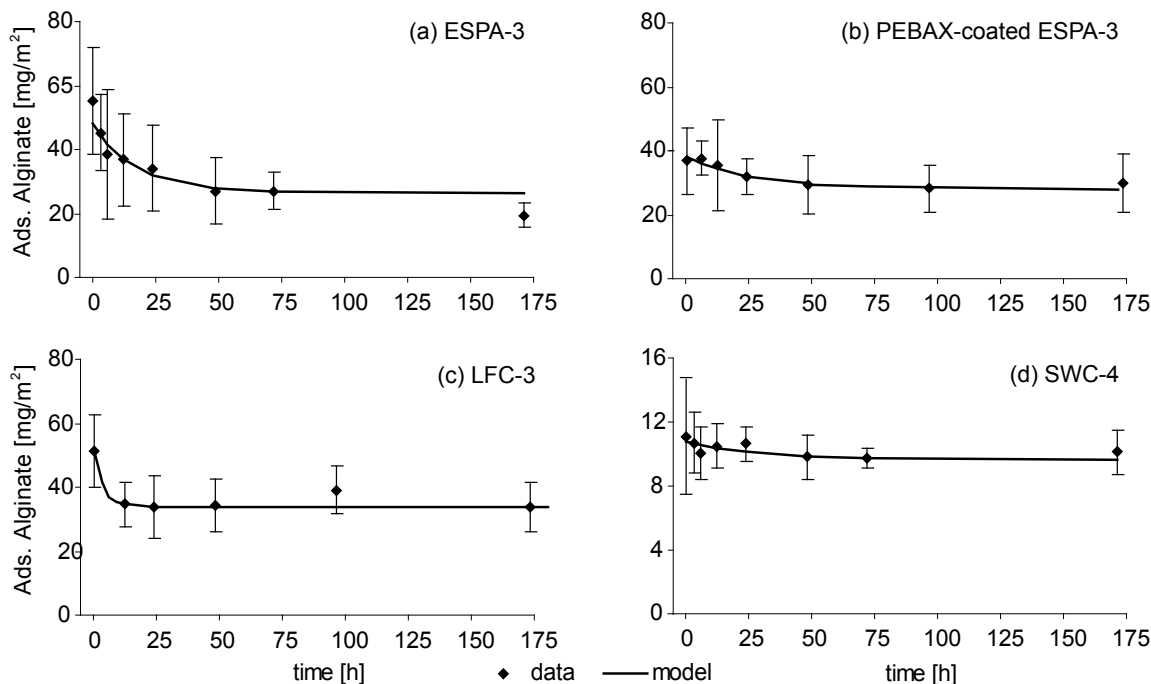


Figure 10: Desorption data from Figure 5 with a first-order desorption model superimposed. The model parameters are as follows (a):  $A_1 = 21.6 \text{ mg/m}^2$ ,  $A_2 = 26.4 \text{ mg/m}^2$ ,  $\tau = 17 \text{ h}$ ; (b):  $A_1 = 10.2 \text{ mg/m}^2$ ,  $A_2 = 27.6 \text{ mg/m}^2$ ,  $\tau = 28 \text{ h}$ ; (c):  $A_1 = 17.2 \text{ mg/m}^2$ ,  $A_2 = 33.8 \text{ mg/m}^2$ ,  $\tau = 3.5 \text{ h}$ ; (d):  $A_1 = 1.3 \text{ mg/m}^2$ ,  $A_2 = 9.4 \text{ mg/m}^2$ ,  $\tau > 30 \text{ h}$ . Note that the scale for (d) has been changed to obtain better resolution.

## 10 Data Summary and Discussion

A summary of the most commonly-measured data point, adsorption of a 1 g/L alginate solution over 24 h, is shown in Figure 11. The final “overall average” values are based on 16 (SWC-4), 24 (ESPA-3) or 32 (LFC-3 and PEBAX-coated ESPA-3) replicates each.

While these results alone are not sufficient to determine which membrane characteristics are important for membrane bio-fouling and will have to be corroborated by cross-flow fouling experiments under the same conditions, they do point to some general trends: First,

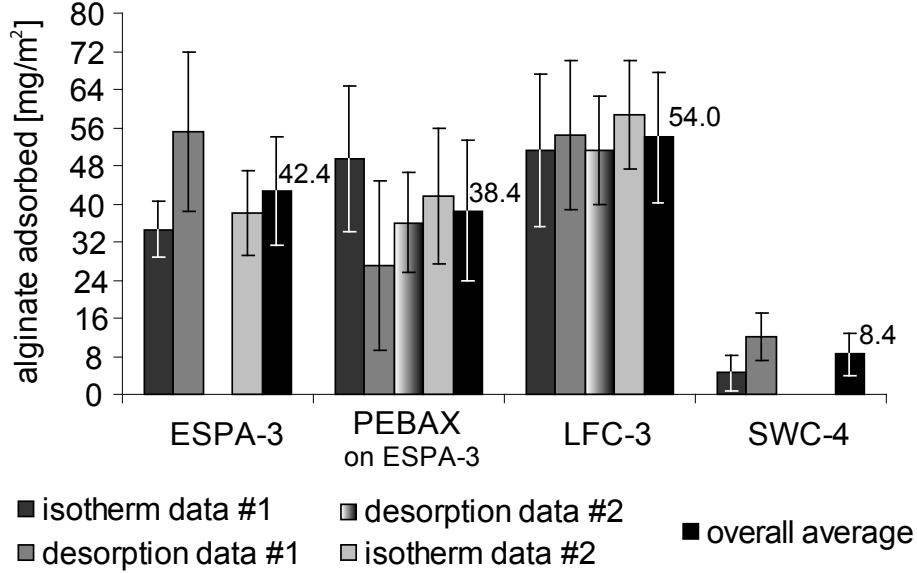


Figure 11: Summary of 24 h adsorption data. The numbers beside the last bar for each membrane shows the numeric value of the “overall average,” an average of all replicates. The error bars indicate one standard deviation.

the ESPA-3, PEBAX-coated ESPA-3 and LFC-3 membranes experienced a similar amount of alginate adsorption (24 h at 1 g/L:  $42.6 \pm 11.4$ ,  $38.5 \pm 14.7$ ,  $53.9 \pm 13.8$ ,  $8.4 \pm 4.4$ , respectively). Surprisingly, LFC-3, which is sold as a low-fouling membrane, consistently showed slightly higher values for adsorption. SWC-4, on the other hand, which is a more selective membrane, showed very little adsorption. The equilibrium results from desorption experiments were equally unexpected, as the low-fouling LFC-3 membrane irreversibly retained even more alginate than any of the other membranes ( $33.8 \text{ mg/m}^2$  versus  $26.4 \text{ mg/m}^2$ ,  $27.6 \text{ mg/m}^2$  and  $9.4 \text{ mg/m}^2$  for ESPA-3, PEBAX-coated ESPA-3 and SWC-4, respectively). Interestingly, the PEBAX coating, which has been shown elsewhere to prevent fouling [7], slightly increases the amount irreversibly adsorbed as compared to the uncoated ESPA-3. Finally, the desorption kinetics showed the most marked differences between the three brackish-water membranes. While the uncoated and PEBAX-coated ESPA-3 had first-order desorption time constant of over 17 h and over 27h, respectively, the approximate time constant for alginate desorption from LFC-3, was only 3 – 4h. This means that the desorption of alginate from LFC-3 membranes was at least an order of magnitude faster than any of the other membranes (for SWC-4,  $\tau > 30h$ ).

Therefore, we conclude that - at least as far as static adsorption studies are concerned - desorption kinetics may be a much better indicator of membrane fouling potential than either the simple adsorption behavior, or the desorption equilibrium. Additionally, the conventional wisdom that surface roughness is the defining factor behind membrane fouling is also questioned by this data, since the PEBAX coating on the ESPA-3 membrane served to make it much smoother than the uncoated version [7], with little or no effect on alginate adsorption or desorption.

# 11 Molecular Modeling Results

## 11.1 Goals and Objectives

A goal of this project was to determine the feasibility of using molecular modeling protocols to simulate alginate adsorption to a model polyamide (PA) membrane surface. Accordingly, modeling efforts were focused on the development of efficient computer algorithms that were capable of automatically building both alginate polymers as well as crosslinked PA membranes. The molecular structure of bacterial alginate varies according to the strain of *Ps. aeruginosa*, the nutrient regime, and a host of other environmental parameters. Thus, the alginate building algorithm needed to be able to account for such variation in a manner that allowed the user of the program to specify a desired set of molecular properties, such as overall charge, the degree of acetylation, monomer ratios, mass, etc. Similarly, the algorithm developed for the creation of model PA membrane fragments also featured the ability to select a suite of desired membrane properties, including the net membrane charge and the degree of aromatic crosslinking. The alginate building and PA membrane building algorithms are described in more detail below.

## 11.2 Polyamide (PA) Membrane Models

The PA membrane models used in this project were prepared using a “3D lattice random-walk” approach. An important assumption in this approach and the basis of model construction is that the two reactive monomer species, m-phenylenedimaine (MPD) and trimesoyl chloride (TMC) are initially present as a perfectly mixed equimolar solution. In actual practice this is of course not the case since the solvent insoluble membrane is produced interfacially at the junction of two immiscible solvent phases. The two monomers are brought into mutual proximity at the liquid-liquid phase boundary where they undergo diffusion mediated mixing followed by extremely rapid condensation (Figure 12).

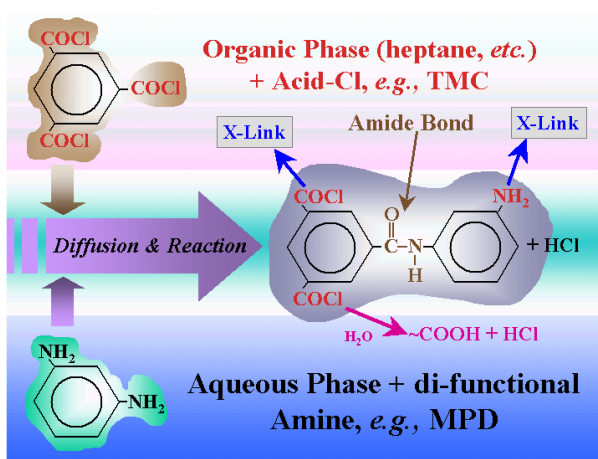


Figure 12: Schematic illustrating the basic steps in the interfacial polymerization reaction in which TMC and MPD react to form an insoluble permselective PA membrane

Under such conditions, asymmetric monomer concentration gradients undoubtedly develop at the liquid interface leading to incomplete monomer mixing. The present generation of membrane-building computer algorithms are not equipped to take these complex mixing effects into account. Exactly how monomer diffusion and mixing occurs at this interface is imprecisely understood. Hence, the extent to which the modeling approach emulates mixing conditions during actual PA membrane synthesis is debatable. All else being equal, a molar imbalance of either monomer resulting from poor interfacial mixing would presumably result in poor chain extension and/or reduced internal (i.e., intra-chain) crosslinking. Thus, an important feature of the computer algorithm is the ability to alter the degree of intra-chain crosslinking over the range from no crosslinking to complete crosslinking. This ability should allow the future exploration of the influence of a range of crosslinking densities on alginate adsorption behavior and other membrane characteristics. As illustrated below, the membrane charge and polymer density (i.e., polymer packing) may also be varied at will.

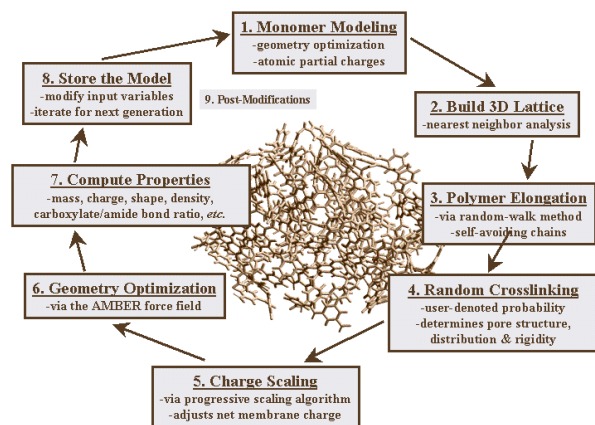


Figure 13: Outline of basic steps in the polyamide membrane building program.

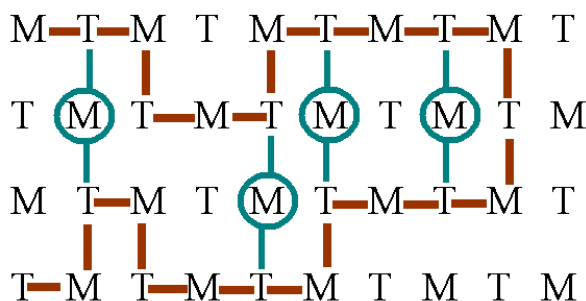


Figure 14: Schematic illustrating a random-walk chain extension (brown line) and subsequent cross linking operations.

The basic steps involved in the PA membrane building program are outlined in Figure 13. In the algorithm developed, a binary monomer "solution" is implemented by building a three-dimensional (3D) cubic lattice (i.e., matrix) of alternating MPD and TMC residues (i.e., monomers). Beginning at the lattice origin point (usually the first monomer placed into the matrix) a "random walk" excursion through the 3D matrix is performed. At each step (i.e., node), MPD and TMC residues undergo bonding (Figure 14). Such chain extension occurs until all available bonding partners are utilized. In this way, a randomly-folded self-avoiding polymer chain is generated. X-ray diffraction analyses have indicated that actual PA membranes exhibit no ordered polymer structure, i.e., no detectable crystallinity at the atomic scale. The random walk, which is equivalent to chain elongation, is self-terminated by the program at "dead end" points when no new unbonded nearest-neighbor partners can be identified.

Following chain extension, TMC residues that by chance fold into proximity to one another are allowed the opportunity to undergo crosslinking by a neighboring and still unbonded (i.e., “free”) MPD residue, if one exists, thereby creating a fully covalently bonded nanoporous polymeric network. As indicated in Figure 15, each crosslink junction serves to define a new nanopore. The shape, dimensions, distribution, reactivity and dynamics of the membrane nanopores are thought to be involved in how solvent (e.g., water) and small solute molecules (e.g., trace organics) gain access to the membrane interior and their subsequent diffusion-based transport across the membrane. The rate of solute diffusion through the membrane determines how well a given compound is rejected. Figure 16 shows the Connally probe surface (calculated for a water probe radius of 1.4 Angstroms) for a geometry-optimized PA membrane model. The probability of intra-chain TMC crosslinking may be adjusted by the user of the program. In order to perform the random-walk chain elongation, a nearest-neighbor analysis must be performed on the 3D lattice. This analysis was done by a rule-based (instead of a distance-based) method to allow improved control of membrane polymer density and to reduce the likelihood of poor atom contacts.

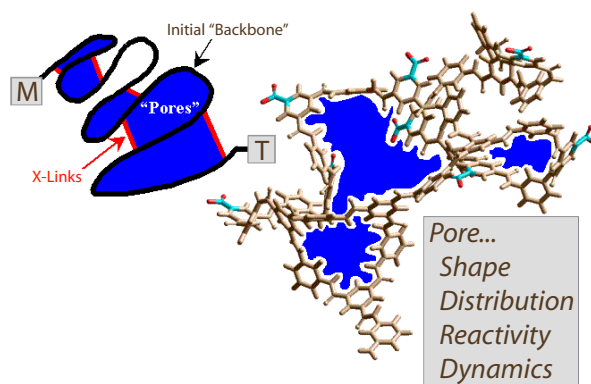


Figure 15: Schematic illustrating the creation of membrane nanopores by crosslinking.

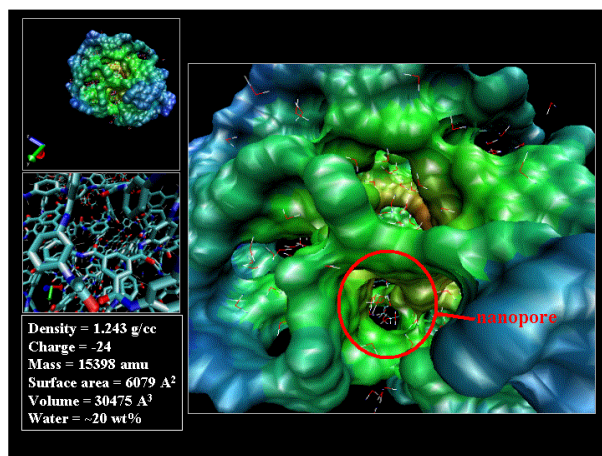


Figure 16: Probe surface of a hydrated polyamide membrane model showing the creation of nano-pores whose spatial distribution and dynamics influence water and solute transport processes.

The membrane model used in this study had a water content of ~20wt%, a mass of 15398 amu, a density of 1.24 g/cc, and a net charge of -24 eV and a crosslink probability of 1.0 that resulted in a carboxylate/amide bond ratio of about 0.25. The carboxylate/amide bond ratio for the membrane model falls within the range observed for actual (commercial) PA membranes as determined by attenuated total reflection Fourier transform infrared spectrometry (Ken Ishida, OCWD, personal communication). The membrane density and other properties closely match the known physicochemical properties of actual PA membranes (Kotelyanskii et al., 1998). A total of 24 sodium atoms (Na<sup>+</sup>), each with a fixed charge of +1.0, were

added randomly to the initial PA membrane model to balance the collective anionic charge of the non-protonated membrane carboxylate groups.

### 11.3 Alginate Modeling

As described before, bacterial alginate is a linear (non-crosslinked) polymer of L-guluronic (G) acid and D-mannuronic (M) acid (Figure 17). It is produced by *Pseudomonas aeruginosa* and certain other bacterial species as an extracellular glycocalyx where it protects the cell from predation and dehydration. The M residues, but not G residues, may or may not be acetylated at the positions shown in Figure 6 depending on specific growth conditions and the genetic makeup of the strain involved. Similarly, alginate chain lengths vary widely across bacterial strains, but molecular weights are generally high, typically ranging from a low value of a few tens of thousands to well over one million Daltons. The ratios of M and G monomers and the frequency of occurrence of GG diads and triads are also dependent on the strain and nutrient conditions.

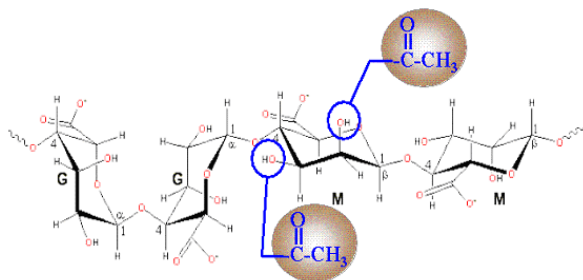


Figure 17: Chemical structure for bacterial alginate. Mannuronic acid residues may be acetylated at the positions shown.

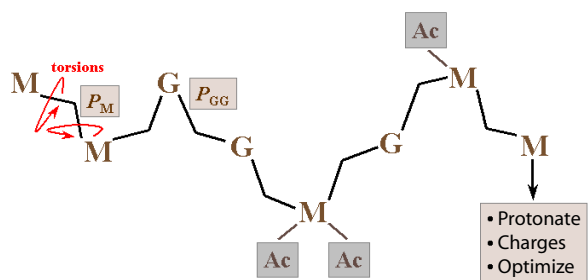


Figure 18: Diagram of primary steps involved in building molecular models of bacterial alginate. See text for details.

A computer algorithm was developed to automatically generate models of bacterial alginate whose monomer ratios and degree of acetylation could be varied over any desired range. The algorithm calculates the probability of generating specified M/G monomer ratios and GG diad frequencies at each step of chain elongation. The probability of random acetylation of mannuronic acid residues is independently calculated in a separate step (see Figure 18). At each monomer addition step, dihedral angles between monomers are optimized to low-energy configurations followed by overall chain relaxation. The degree of dihedral angle relaxation is specified by the user of the program as one of the initial setup variables. All alginate parameters, e.g., chain length, charge, monomer ratios, etc. may be varied incrementally or randomly over a population of alginate polymers that are requested. The specific alginate model used in this project is shown in Figure 19. With the exception of the short chain length consisting of eight alternating M/G monomers, the calculated properties of this model were similar to actual bacterial alginate. Since the net charge of the alginate model was -8.0 eV, an equal number of  $\text{Na}^+$  counterions were used to maintain charge neutrality of

the model. In preparation for molecular dynamics simulations (see below), a 3.0 Å shell of water molecules ( $\sim 55M$ ) were randomly added to better simulate the effects of hydration.

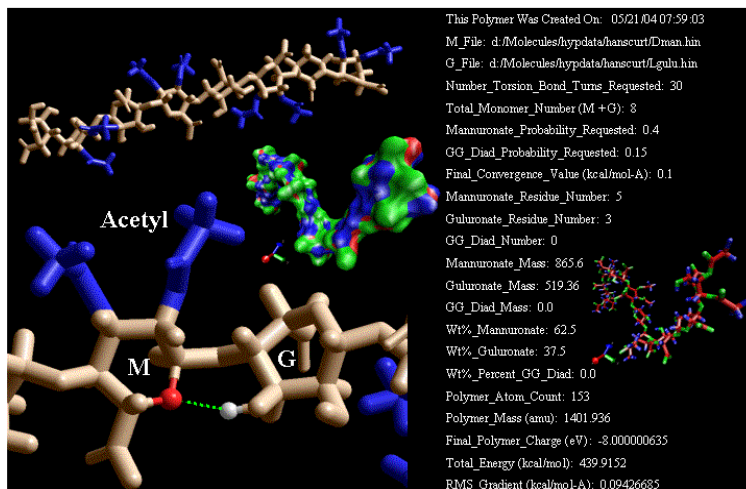


Figure 19: Alginic acid Model #501 selected for use in this project. An M/G intrachain hydrogen bond is indicated by the dashed green line. Acetyl groups are colored blue. The space-filled Connolly surface rendition (1.4 Å probe diameter) of this alginic acid model is also shown. With the exception of the short chain length, the overall properties of this model are typical of actual bacterial alginate from *P. aeruginosa*.

## 11.4 Molecular Dynamics (MD) Simulations

The above alginate and membrane models were combined into a single molecular system to simulate how bacterial alginate might undergo adsorption to a typical PA membrane surface. Various views of this molecular system are depicted in Figure 20. The alginate polymer was randomly positioned approximately 20 Å “above” the fully hydrated membrane model under rectangular periodic boundary conditions (35x200x40 Å). The simulation was run for an uninterrupted period of  $\sim 300$  psec ( $\sim 0.3$  ns) at a constant temperature of 300K. Other run parameters are summarized in Table 1.

MD Run Temperature	300 °K, constant
Periodic Boundaries	35 x 200 x 40 Å
Cutoff boundaries (switched)	17.5 Å <sub>outer</sub> ; 13.5 Å <sub>inner</sub>
MD Run Time	$\sim 300$ psec (0.3 ns)
Force Field for Simulations	Amber 99
Dielectric	constant (at 1.0 scale factor)
Electrostatic 1-4 scale factor	0.833
VDW 1-4 scale factor	0.5

Table 1: MD run conditions used in this project

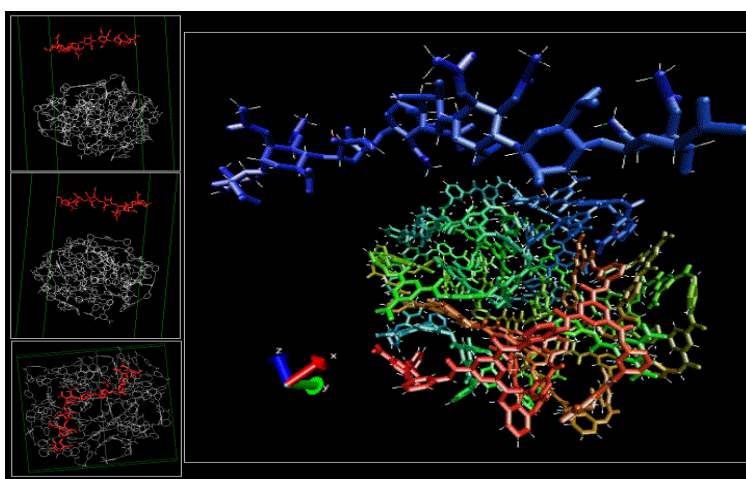


Figure 20: Molecular system used for MD simulations. The system is shown at  $t = 0$ , i.e., at the beginning of the simulation. To better illustrate the polymer network, water molecules and sodium ions have been omitted. The left-hand panels indicate the initial orientation of the molecules. The right-hand panel is a perspective view of the system looking obliquely down the vertical system axis (not shown).

## 11.5 Simulation Results

Throughout the run period of  $\sim 300$  psec, the alginate chain gradually underwent “adsorption” to the PA membrane surface (see Figure 21). Alginate adsorption was quantified by the center-of-mass separation distance between the alginate chain and the PA membrane. Initial alginate adsorption appeared to be more-or-less completed by about 200 psec of elapsed time, although the polymer continued to undergo subtle rearrangements throughout the run period. Adsorption throughout the  $\sim 300$  psec run time was associated with a decline in the overall system potential energy suggesting the adsorbed state was more energetically favorable than the “desorbed” condition (Figures 22 and 23). Monitoring of the interaction potential between the alginate polymer and the water/Na+/membrane “complex” suggested that Van der Waals interactions became increasingly significant as the polymer underwent adsorption to the membrane surface (see Figure 24). Electrostatic interactions were least significant at about 200 psec into the simulation.

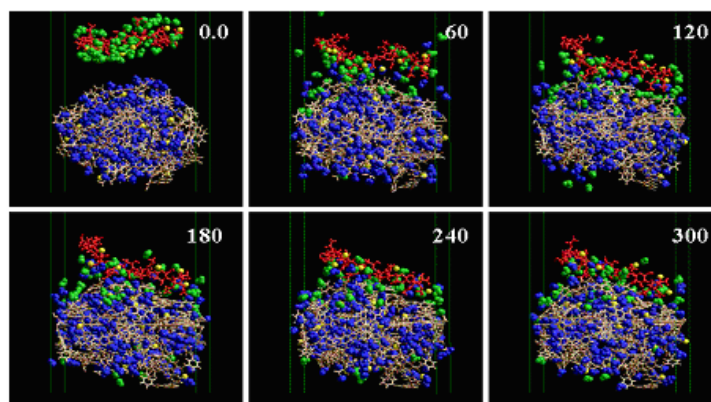


Figure 21: Series of image captures showing the progress of alginate (red) adsorption to the model PA membrane surface (brown). Water molecules initially associated with the alginate chain are colored green. Membrane water molecules are blue. Sodium ions are yellow. Frame numbers indicate number of elapsed psec.

Figure 25 depicts the overall (b, c) and corresponding detail views (a, d) of the alginate polymer following adsorption to the membrane surface ( 300 psec). These images suggest that the alginate and membrane polymer chains undergo mutual low-energy conformational rearrangements that result in a kind of “dovetailing” of the surfaces. Van der Waals interactions might be expected to be enhanced under these “close contact” circumstances relative to electrostatic forces. Although not quantified at this time, the positioning of the acetyl groups proximal to membrane atoms suggests that they might be involved in stabilizing alginate adsorption, perhaps through hydrophobic interactions. Additional experimental and modeling analyses using non-acetylated alginate should be performed to confirm this hypothesis.

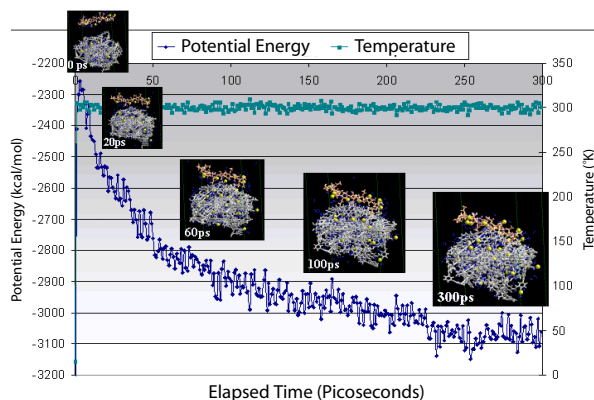


Figure 22: System temperature and potential energy during the MD run. Brown = alginate chain; gray = PA membrane; blue = water; yellow = sodium ions.

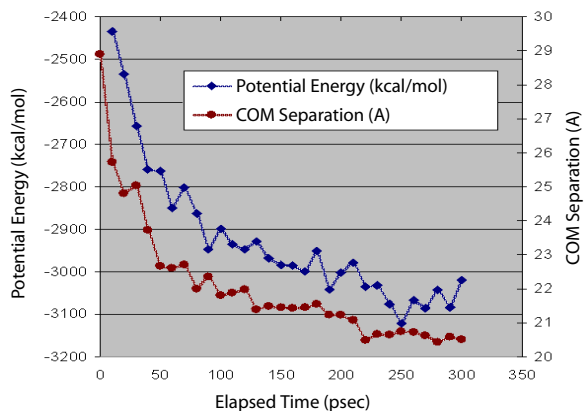


Figure 23: System potential energy and center-of-mass separation between the alginate polymer and the membrane during the MD run.

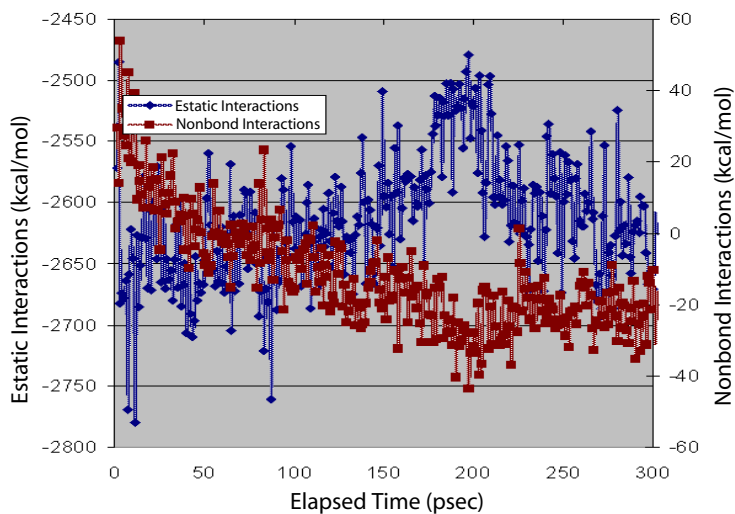


Figure 24: Electrostatic (Estatic) and Van der Waals (i.e., non-bonded) contributions to the calculated interaction potential between the alginate polymer and the water/ $\text{Na}^+$ /membrane complex. Note that as the alginate undergoes adsorption, the non-bond contributions become more significant.

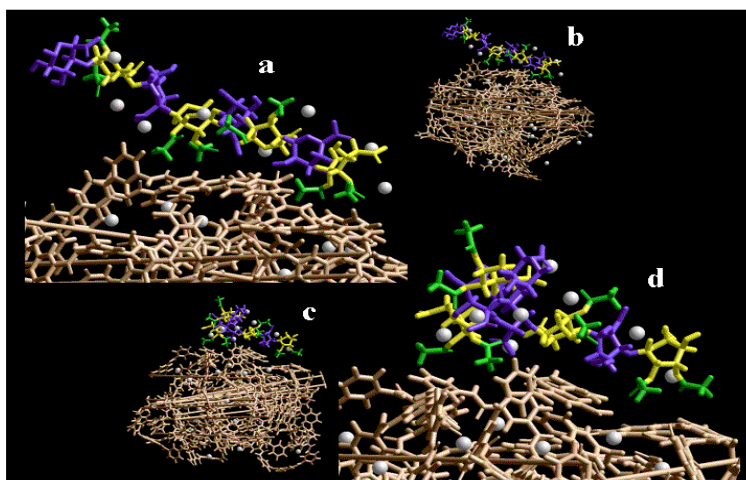


Figure 25: Overview (b, c) and detail (a, d) images of adsorbed alginate captured at  $\sim 300$  psec. Water molecules have been eliminated to enhance visualization of the interaction between the alginate and the membrane surface. Green = acetyl groups; blue = guluronic acid residues; yellow = mannuronic acid residues; white =  $\text{Na}^+$  ions; brown = PA membrane.

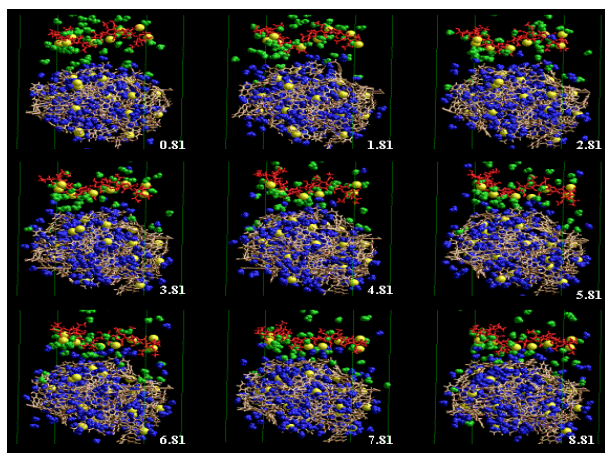


Figure 26: Alginate adsorption during the initial  $\sim 9$  psec of MD simulation. Note that water molecules initially associated with the alginate polymer are rapidly adsorbed onto the PA membrane “surface” during this early phase of the simulation.

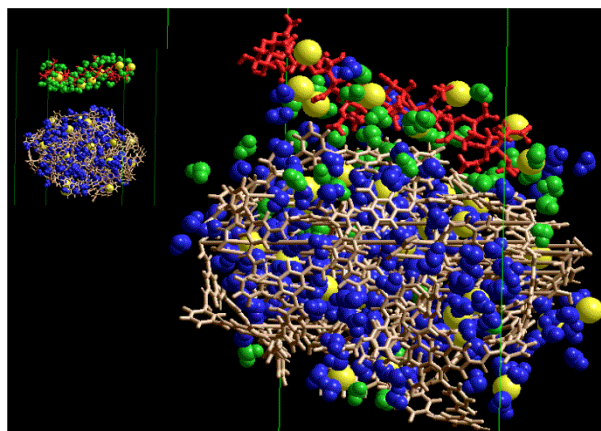


Figure 27: Initial ( $t = 0$  psec, left) and final ( $t = \sim 300$  psec, right) arrangements of water molecules (green) initially associated with alginate (red) and those (blue) initially associated with the membrane (brown).

Figures 26 and 27 depict, respectively, (i) an image sequence captured during the initial 9 psec of the MD simulation and (ii) a close up view of the first and last MD frames. Water molecules initially associated with the polymer are color coded green allowing them to be visually tracked throughout the simulation. These images indicate that the alginate polymer was partially dehydrated very early in the MD simulation, suggesting that water is intimately involved in overall alginate adsorption dynamics. Although not pursued in this study, additional modeling exercises could be used to explore the water exchange behavior and kinetics between alginate and the PA membrane matrix. Such theoretical calculations could be useful in determining how membrane water fluxes might be influenced by adsorbed bacterial alginate and other polymeric foulant species.

## 12 Conclusions

Our original hypothesis was that there would be some sort of correlation, perhaps linear, between membranes rate of bio-fouling under operational conditions and the amount of alginate they adsorbed. This turned out not to be the case, in fact, LFC-3, which is sold as a lower-fouling membrane than ESPA-3 and SWC-4 adsorbed more than both membranes. Even more remarkably, SWC-4, which has similar fouling tendencies as well as surface properties to ESPA-3 [7] adsorbs up to ten times less material.

However, the results from our desorption studies showed some more promise. Despite the fact that all the membranes showed more than 50% irreversible sorption of alginate under static conditions, the kinetic data showed an order of magnitude higher desorption rate for LFC-3, which leads us to our new working hypothesis that the bio-fouling potential of a membrane may be better characterized by its desorption behaviour than its adsorption behaviour. This hypothesis is as yet untested, but will guide us in further investigations.

Finally, molecular modeling tools show promise in predicting some aspects of alginate adsorption behavior. Representative structures for both polyamid membranes and bacterial alginate were constructed in the model environment. Model runs allowing contact between these two structures showed an overall drop in system energy upon alginate adsorption, which is consistent with the experimental findings of this study, particularly in the context of the large fractions of irreversible adsorption. Further model investigations into the effect of alginate and membrane structures may give us useful insights into the mechanism of alginate attachment, which will lead to a greater understanding of biofouling in general.

## 13 Recommendations for Future Work

The *Pseudomonas aeruginosa* FRD1153 strain (an AlgJ knockout mutant) that is designed to produce non-acetylated alginate does not seem to be very mucoid. It is likely that the strain shut down the alginate production pathway again before I was able to create stock cultures. One possible way to make sure of this would be to plate one culture from each stock vial to see if there are, per chance, some stock vials that are more mucoid than others. This would cost a lot of material and create a lot of waste, so it should be considered carefully. Another option is to use alginate from the wild type strain (FRD1) and chemically deacetylate the alginate following a procedure provided by Mike Franklin. This procedure would take a while to set up, but should be more reliable than hoping for the FRD1153 mutant to start producing alginate.

With all the difficulty relating to  $^{14}\text{C}$  labeling, different methods for visualizing, and perhaps quantifying sorbed alginate concentrations were explored. One option that has presented itself is fluorescence labeling. A very quick literature search produced a variety of options, including several direct references for fluorescence-labeling of alginates. One reference even discussed labeling alginates harvested from *Pseudomonas aeruginosa* [10].

The next logical steps in this project are outlined in the project proposal. Following more adsorption experiments to confirm isotherm and kinetic behavior, desorption kinetics as well as the effects of interferences such as surfactants, other sugars/carbohydrates or salt will be studied.

Additionally, surface characteristics such as surface charge and roughness, of the membranes used in the adsorption experiments will be determined in order to search for correlations between the two data sets. The hypothesis supported by current literature is that the rougher a surface, the more quickly it will foul. The data collected with the adsorption experiments will be a first set of truly quantitative measurements to either confirm or refute this line of thought.

Finally, should this project be extended beyond the current expiration date, a completely new set of experiments using larger membrane coupons and a flow-through cell could be conducted. These would consist of pre-fouling membrane coupons using a similar approach as the microtiter tests, but on a larger scale. Since the total mass of alginate adsorbed per unit area could be extrapolated from the experiments currently underway, using labeled alginate would not be necessary. This would simplify the administrative aspect of these experiments substantially. The pre-fouled membranes could then be placed in a flow-through apparatus, and tested according to the standard membrane performance metrics, specific flux and rejection. This would provide an additional first truly quantitative correlation between the foulant mass adsorbed on and the performance degradation of the membranes.

The procedures developed so far open the door to a range of novel research opportunities and we are planning to submit a proposal for follow-up work. The objectives of this proposal will be:

1. Develop sorption isotherms with flow cell-sized membrane coupons (4" x 6");
2. Develop performance data as a function of membrane coverage;
3. Evaluate sorption as a function of water quality;
4. Develop alternative methods of quantifying sorption and distribution of EPS materials;
5. Study the stability of the adsorbed materials under water treatment conditions;
6. Study the efficacy of cleaning procedures;
7. Study the biological formation of EPS and its significance for membrane performance.
8. Explore the potential of molecular modeling to explain and predict fouling effects of EPS and other polymers on the performance of polyamid membranes.

## References

- [1] P. Campbell, R. Srinivasan, T. Knoell, D. Phipps, K. Ishida, J. Safarik, T. Cormack, and H. Ridgway. Quantitative structure-activity relationship (qsar) analysis of surfactants influencing attachment of a mycobacterium sp. to cellulose acetate and aromatic polyamide reverse osmosis membranes. *Biotechnology and Bioengineering*, 64(1):61–67, January 1999.
- [2] H.-C. Flemming. Biofouling in water systems cases, causes and countermeasures. *Applied Microbiology and Biotechnology*, 59:629–640, 2002.
- [3] M. Franklin. Preparation of alginate for bioadhesive studies. obtained through personal communication.
- [4] M. Franklin and D. Ohman. Mutant analysis and cellular localization of the algI, algJ, and algK proteins required for O acetylation of alginate in pseudomonas aeruginosa. *Journal of Bacteriology*, 184(11):3000–3007, 2002.
- [5] P. Gerhardt, R.G.E. Murray, R.N. Costilow, E.W. Nester, W.A. Wood, N.R. Krieg, and G.B. Phillips, editors. *Manual of Methods for General Bacteriology*, pages 333–334. American Society for Microbiology, 1981.
- [6] Saha K.S. and C.F. Brewer. Determination of the concentrations of oligosaccharides, complex type carbohydrates, and glycoproteins using the phenol-sulfuric acid method. *Carbohydrate Research*, 254:157–167, 1994.
- [7] J. S. Louie, I. Pinnau, I. Ciobanu, K.P. Ishida, A. Ng A., and M. Reinhard. The effects of polyether-polyamids block copolymer coating on performance and fouling of reverse osmosis membranes. *Journal of Membrane Science*, 2006. in press.
- [8] Dubois M., Gilles K.A., Hamilton J.K., Rebers P.A., and Smith F. Colorimetric method for determination of sugars and related substances. *Anal Chem*, 28:350–356, 1956.
- [9] D. Nivens, D. Ohman, J. Williams, and M. Franklin. Role of alginate and its O acetylation in formation of pseudomonas aeruginosa microcolonies and biofilms. *Journal of Bacteriology*, 183(3):1047–1057, 2001.
- [10] Berit L. Strand, Yrr A. Mrch, Terje Espevik, and Gudmund Skjk-Brk. Visualization of alginate-poly-L-lysine-alginate microcapsules by confocal laser scanning microscopy. *Biotechnology and Bioengineering*, 82(4):386–394, March 2003.
- [11] Kai M. Thormann, Rene M. Saville, Soni Shukla, Dale A. Pelletier, and Alfred M. Spormann. Initial phases of biofilm formation in shewanella oneidensis mr-1. *Journal of Bacteriology*, 186(23):8096–8104, December 2004.